The Frequency Response of Smooth Muscle Stiffness during Ca^{2+}-Activated Contraction

Guay-haur Shue and Frank V. Brozovich
Department of Medicine (Cardiology) and Department of Physiology and Biophysics, Case Western Reserve University, Cleveland, Ohio 44106 USA

ABSTRACT To investigate the mechanism of smooth muscle contraction, the frequency response of the muscle stiffness of single β-escin permeabilized smooth muscle cells in the relaxed state was studied. Also, the response was continuously monitored for 3 min from the beginning of the exchange of relaxing solution to activating solution, and then at 5-min intervals for up to 20 min. The frequency response (30 Hz bandwidth, 0.33 Hz (or 0.2 Hz) resolution) was calculated from the Fourier-transformed force and length sampled during a 3-s (or 5-s) constant-amplitude length perturbation of increasing-frequency (1–32 Hz) sine waves. In the relaxed state, a large negative phase angle was observed, which suggests the existence of attached energy generating cross-bridges. As the activation progressed, the muscle stiffness and phase angle steadily increased; these increases gradually extended to higher frequencies, and reached a steady state by 100 s after activation or ~40 s after stiffness began to increase. The results suggest that a fixed distribution of cross-bridge states was reached after 40 s of Ca^{2+} activation and the cross-bridge cycling rate did not change during the period of force maintenance.

INTRODUCTION

In smooth muscle, contraction is primarily initiated through the phosphorylation of the 20-kDa myosin light chain (MLC) by Ca^{2+}-calmodulin-dependent MLC kinase (Hartshorne, 1987; Kamm and Stull, 1985), whereas relaxation occurs via the dephosphorylation of the MLC by a MLC phosphatase (Bialojan et al., 1987; Haeberle et al., 1985). However, for many types of stimuli, force is maintained after intracellular Ca^{2+} and MLC phosphorylation fall from the high level reached during force development. This has been referred to as the latch state (Dillon et al., 1981; Hai and Murphy, 1988) and its molecular mechanism is not fully understood. The unloaded shortening velocity (V_{max}) of smooth muscle also decreases during force maintenance (Dillon and Murphy, 1982; Moreland et al., 1987). This decrease in V_{max} has been suggested to be due to the presence of non/slowly cycling latch cross-bridges (Hai and Murphy, 1988), or an overall slowing of the entire cross-bridge cycling rate (Butler et al., 1986).

In this study the two hypotheses above were assessed by studying the frequency response of the muscle stiffness of single smooth muscle cells during force activation and force maintenance. The frequency response (i.e., stiffness and phase spectrums) calculated from the force response and length stimulus reveals the characteristics of a muscle. An increase in the stiffness indicates an increase in the number of attached cross-bridges, and a positive phase (force leads length) in the phase spectrum indicates the attached cross-bridges are consuming energy, while a negative phase (force lags length) indicates the cross-bridges are generating energy (Kawai and Brandt, 1980). The profile or shape of the stiffness and phase spectrums suggests the minimum number of exponential processes (cross-bridge groups) and the rates and composition of these processes (Kawai and Brandt, 1980).

The results from this technique, or the profiles of stiffness and phase angle versus the frequency of oscillation, are also sensitive to changes in the cross-bridge cycling rate. If the cross-bridge cycling rate slows, the profiles of the stiffness and phase spectrums will shift to the left, to lower frequencies, or the extent of the profiles will decrease. If the cross-bridge cycling rate increases, the stiffness and phase spectrum will shift to the right, to higher frequencies, or the extent of the profiles will increase.

Kawai's group has used fixed-frequency sinusoidal length perturbations to obtain the frequency responses of skeletal muscle fibers (Kawai and Brandt, 1980; Wang and Kawai, 1996) and myocardium (Kawai et al., 1993). However, the method is only good for steady-state studies since it requires a large number of measurements to construct a frequency response plot. To study the time course of frequency response from the beginning of muscle contraction, a method with good temporal resolution is required.

For this study, a length perturbation sequence that combines multiple sine waves with increasing frequency was developed. The 3-s (or 5-s) sequence was Fourier-transformed to a frequency response with 30 Hz bandwidth and 0.33 Hz (or 0.2 Hz) resolution. With the sequence, we found large negative phase angles at lower frequencies in the phase spectrum of relaxed cells, which suggests the existence of a population of energy-generating attached cross-bridges. These negative phase angles also existed in the phase spectrum of activated cells, suggesting that these attached cross-bridges may contribute to force in the active

Received for publication 19 August 1998 and in final form 17 February 1999.

Address reprint requests to Dr. Frank V. Brozovich, Department of Physiology and Biophysics, Case Western Reserve University, 10900 Euclid Ave., Cleveland, OH 44106-4970. Tel.: 216-844-8955; Fax: 216-368-5586; E-mail: fxb9@po.cwru.edu.

0006-3495/99/05/2361/09 $2.00

state as well. Also, the frequency response, which was continuously monitored from the beginning of muscle contraction, showed that the increases in the stiffness and phase angle reached a steady state early during force activation and did not change during force maintenance.

METHODS

Cell preparation

Single vascular smooth muscle cells (VSMCs) were enzymatically isolated from the portal vein of New Zealand White rabbits using a previously described method (Brozovich and Yamakawa, 1995). The vessel was cut into small (~1 mm^2) pieces, and then transferred to Hanks' solution in a siliconized flask containing CLS II collagenase, type IV elastase, and type II-S trypsin inhibitor. Four incubations were performed at 37°C under 95% O_2–5% CO_2 in a shaking water bath at 80 cycles/min and the pieces were filtered and rinsed on a nylon mesh after each incubation. The dissociated cells were stored on ice for 1–4 h until they were used.

The coverslip containing the intact VSMCs was transferred to a chamber on the movable stage of a Nikon inverted microscope (Fig. 1). The cells were first bathed in relaxing solution (pCa 9, 5 mM MgATP). A healthy VSMC was chosen and its two ends were attached to pulled glass capillary tubes with glue (Polycel, Macklanburg-Duncan, Oklahoma City, OK). One of these capillary tubes was connected to a force transducer (Cambridge 406A, Cambridge Technology, Watertown, MA) in series with a length driver (P-841.20, Physic Instrument, Waldbronn, Germany). Resonant frequency of this system is 50 Hz. To record force and change length, the end of the cell attached to the force transducer/length driver was lifted. The plasma membranes of the VSMCs were permeabilized by a 5-min incubation in relaxing solution containing 30 μg/ml β-escin. Cells were activated by changing the bathing solution to activating solution (pCa 4, 5 mM MgATP).

Solutions

Calcium buffers were mixed according to an iterative computer program that calculates for a given set of free ion concentrations, the amount of stock solutions to be mixed (Brozovich and Yamakawa, 1995). Binding constants for the ionic species present were corrected for both temperature and ionic strength. The experiments were performed at room temperature (22°C). Solutions had 5 mM EGTA ([ethylenebis-(oxyethylenenitrilo)]tetraacetic acid), 1 mM free Mg^{2+}, and 25 mM creatine phosphate. Twenty-five mM BES (*N,N*-bis-(2-hydroxyethyl)-2-aminoethanesulfonic acid) was used for a pH 7.0 buffer, and methanesulfonic acid supplied the major anion. Ionic strength was set at 0.2 M. Solutions were mixed for pCa 4 (activating solution) and pCa 9 (relaxing solution); both solutions contained 5 mM MgATP. Rigor solution contained neither MgATP nor creatine phosphate. Low ADP rigor solution was rigor solution with 50 μM MgADP. For ATPγS relaxing solution, ATP was replaced with ATPγS and creatine phosphate was omitted. The Hanks' solution consisted of (in mM): NaCl, 137; KCl, 5.4; KH_2PO_4, 0.44; NaH_2PO_4, 0.42; $NaHCO_3$, 4.17; HEPES (4-(2-hydroxyethyl)-1-piperazineethanesulfonic acid), 10.0; pH 7.0.

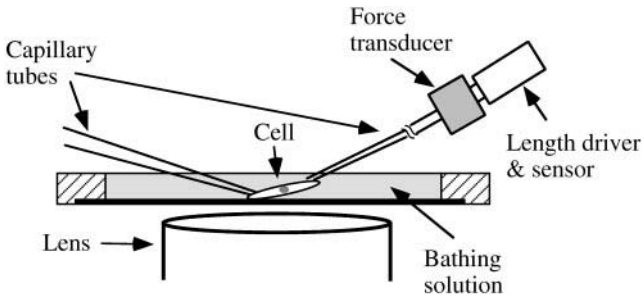

FIGURE 1 The experimental setup. The ends of a cell were attached to two capillary tubes and the end attached to the force transducer/length driver was lifted up. Cells were activated by exchanging bathing solution from relax to active.

Increasing frequency sinusoidal sequence

The length perturbation sequence combined single cycles of sine waves from 1 to 32 Hz in 1-Hz increments (Fig. 2 *A*). The amplitude of the sine waves was constant. The beginning and the end of the combined sine wave sequence were padded with 0.06 and 0.272 s of zeros, respectively, to make the sequence duration 5 s. After Fourier transform, the sequence yielded a length spectrum with 30 Hz bandwidth and 0.2 Hz resolution. However, the amplitude of the length spectrum was too low for frequencies higher than 20 Hz, which caused large ripples in the frequency response of muscle stiffness. Also, since the amplitude of the force spectrum was relatively low at frequencies ranging from 4 to 20 Hz (Fig. 2 *B*), the amplitude of the length spectrum for frequencies higher than 20 Hz should be kept relatively low to enhance the force spectrum at this range. Therefore, the number of cycles of sine waves with frequencies higher than 26 Hz was increased to four. The power spectrum of the sequence is shown in Fig. 2 *B*. The peak-to-peak amplitude of the sequence was chosen as 1.2 μm, which is ~0.6–0.8% of cell length. The amplitude is within the range of the cross-bridges' abilities to remain attached. This was confirmed by calculating the stiffness of single Ca^{2+}-activated skinned cells from the force response to a 15-Hz sinusoidal length change of varying amplitude. Stiffness was constant for amplitudes between 0.3 and 2 μm, and then decreased for amplitudes greater than 2 μm, which indicates a length change >2 μm (~1–1.3% of cell length) broke some attached cross-bridges. During the period of force activation, the frequency response was monitored continuously and a 3-s sequence (0.33 Hz frequency resolution) was used to increase the temporal resolution.

We also examined the applicability of a pseudo-random white noise length perturbation. The amplitude of the sequence was randomly generated between 0.5 and 1 μm every 0.02 s, and linearly interpolated between each point. The sequence was 3 s in length. In comparison to the increasing-frequency sinusoidal sequence, the profiles of stiffness and phase spectrums were similar, but the amplitudes of fluctuations, or noise, in the recorded force sequence and Fourier-transformed force spectrum were doubled.

Data acquisition and processing

As shown in Fig. 2 *A*, the force and length of a cell were sampled at 250 Hz during length perturbation and transformed to Fourier series. Then the force was divided by the length and the resulting complex numbers were converted to the polar form to obtain the stiffness and phase spectrums. The stiffness and phase spectrums displayed in Fig. 2 *A* were obtained when no cell was attached; they represent the frequency response of the vibration of the capillary tube attached to the force transducer. The stiffness increased linearly with frequency for frequencies higher than 10 Hz. The phase angle decreased linearly with frequency, which suggests that there is a constant time delay between the length perturbation and force response.

During the force steady state, relaxed state, or passive state, the 5-s length perturbation was applied, and the resultant frequency response was averaged over five consecutive trials (25 s total) to reduce the influence of noise on the recorded data. Moreover, the data points with standard deviation larger than 0.03 N/m and 30° for stiffness and phase angle, respectively, were removed and interpolated. To study the time course of cross-bridge cycling from force activation to force maintenance, the 3-s length perturbation was continuously applied and data were continuously recorded for 3 min from the beginning of the exchange of relaxing solution to activating solution. To maintain a better temporal resolution during the period of continuous monitoring, the frequency responses were not averaged, but rather smoothed by the 10-point binomial method. Then, during

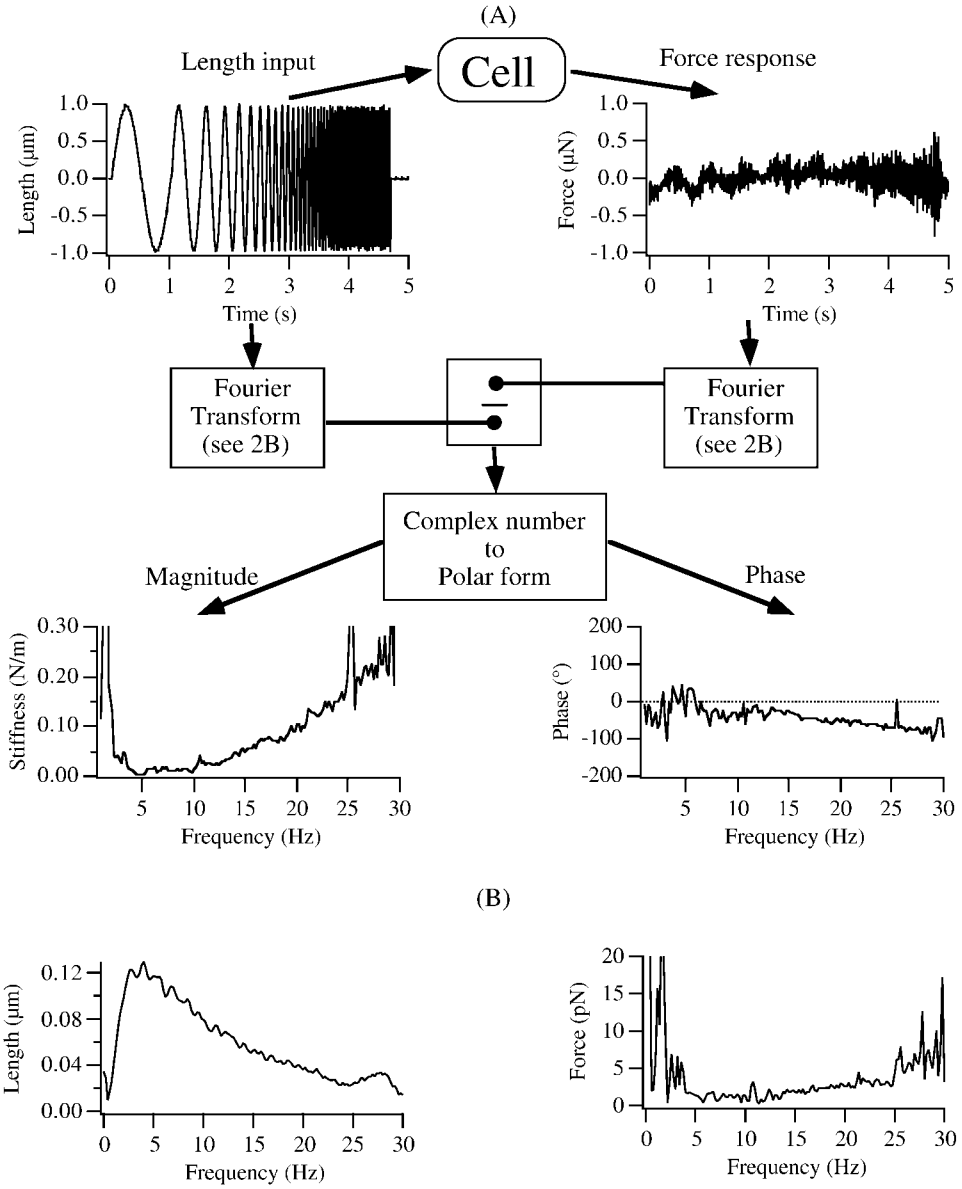

FIGURE 2 (*A*) Typical force and length sequences and the stiffness and phase spectrums when no cell was attached. The stiffness and phase spectrums were calculated from the Fourier-transformed force and length sequences. (*B*) The power spectrums of length and force sequences.

the force steady state, five consecutive 5-s length perturbations were applied at 5-min intervals for up to 20 min, and the recorded data were processed as described above.

Finally, to eliminate the frequency response of passive components, the frequency response of the passive state was used as a reference for the frequency responses of the relaxed and active states. The passive state was produced after all measurements of a cell in the relaxed and active states. The cell was relaxed and stretched (>20% of cell length) several times to break all attached cross-bridges and then the frequency response of the passive state was recorded.

In-phase and quadrature stiffness

For some experiments, stiffness was determined at a single frequency of oscillation. For these experiments, the stiffness was calculated from the force response to a small amplitude (~0.5% of cell length) 4.75-Hz sinusoidal length perturbation (Brozovich and Yamakawa, 1995). The complex stiffness was then separated into two parts: a real part, or in-phase stiffness, and an imaginary part, or quadrature stiffness (Goldman et al., 1984 a, b). For these experiments, the single cells were permeabilized with a 5-min incubation in relaxing solution containing 250 units/ml *Staphylococcus aureus* α-toxin (Brozovich and Yamakawa, 1995).

RESULTS

Passive state

Fig. 3 *A* shows the typical mean and standard deviation of the frequency responses of five consecutive trials in the passive state. The frequency responses of the consecutive trials were very consistent for frequencies between 4 and 25 Hz and between 15 and 29 Hz for the stiffness and phase angle, respectively. The monotonic decrease of phase angle with frequency was similar to the measured phase spectrum when no cell was attached (Fig. 2 *A*). This suggests that there is a constant time delay between the length stimulus and the force response, and that there were no active processes (attached cycling cross-bridges) within the cell. The

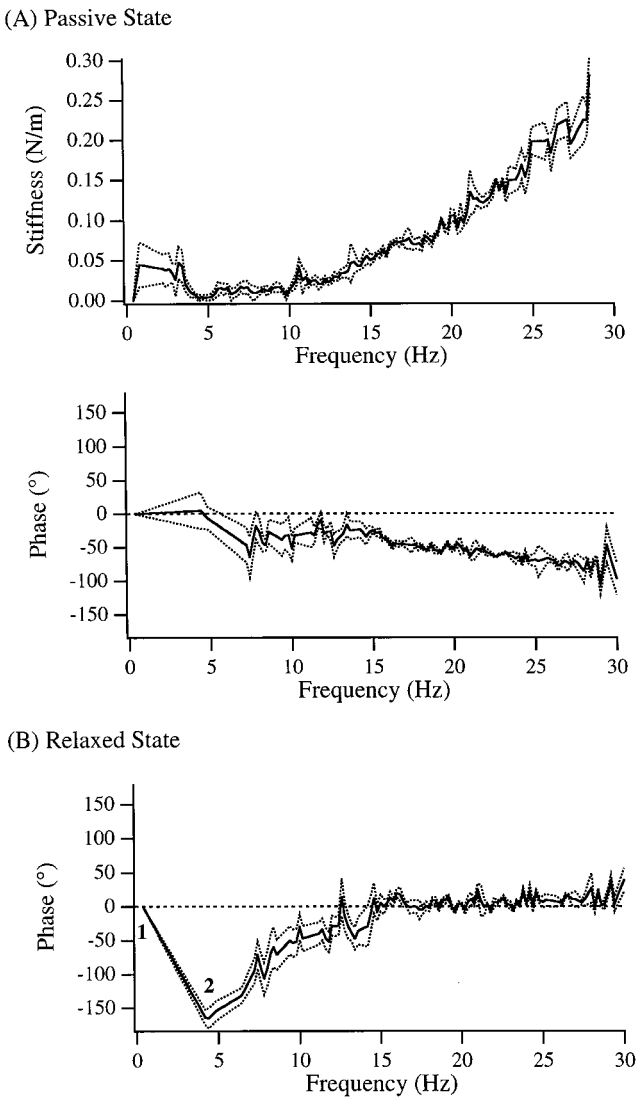

FIGURE 3 (*A*) The mean (*solid line*) and standard deviation (*dotted lines*) of the stiffness and phase spectrums in the passive state. The stiffness and phase spectrums in the passive state are the averages of five consecutive trials and the data points with standard deviations larger than 0.03 N/m and 30° for stiffness and phase angle, respectively, were removed and interpolated. (*B*) The mean and standard deviation of the phase spectrum in the relaxed state, which were calculated from four cells.

frequency response of the passive state should represent the sum of the frequency responses of all passive elements (e.g., force transducer and length driver).

Relaxed state

In comparison with the passive state, stiffness was similar, but there were large negative phase angles at lower frequencies (Fig. 3 *B*). The mean and standard deviation of phase angles were calculated from four cells. The phase angle decreased to −160° at ~4 Hz and then increased to 0° at ~15 Hz then stabilized. The profile of the phase spectrum indicates the existence of at least two exponential processes (Kawai and Brandt, 1980), shown by the marks (1 and 2) on Fig. 3 *B*. The second process shows a phase delay between length and force, which suggests that muscle generates energy at these frequencies. Therefore, attached cross-bridges that generate energy exist in relaxed cells, though there was no detectable stiffness increase caused by these cross-bridges. It may be that the total number of attached cross-bridges is too small to detect an increase in stiffness with our measurement system. However, the phase angle reflects the additional response time caused by the attached cross-bridges and is relatively independent of the number of attached cross-bridges. Thus, despite the low number of attached cross-bridges, a phase angle was detected.

To further investigate whether a population of attached cross-bridges exists in relaxed cells we performed experiments with fixed frequency sinusoidal length perturbation. First, we exchanged the bathing solution of permeabilized cells from relaxing solution to low ADP rigor solution (n = 6). At the release of low ADP rigor solution, the quadrature stiffness, in-phase stiffness, and force of a cell increased and plateaued at ~10 s; then quadrature stiffness and in-phase stiffness started decreasing and stabilized at ~20 s (Fig. 4 *A*). The increases of quadrature stiffness, in-phase stiffness, and force may have resulted from the cooperative reattachment of the attached cross-bridges (Somlyo et al., 1988) that exist in relaxed cells.

To more clearly demonstrate the existence of a population of attached cross-bridges in relaxed cells, relaxed muscle cells were incubated in ATPγS relaxing solution. ATPγS should force all cross-bridges into detached states since it is a substrate for myosin light chain kinase (MLCK), but not for actomyosin ATPase. Therefore, ATPγS will bind to myosin but is not hydrolyzed (Goody and Hofmann, 1980). After incubation in ATPγS relaxing solution (n = 9), transferring cells to low ADP rigor solution resulted in increased in-phase stiffness, but no changes in quadrature stiffness or force were observed (Fig. 4 *B*).

Active state

After the exchange of relaxing solution with activating solution, the frequency response of muscle stiffness was continuously monitored during increasing-frequency sinusoidal length perturbation. The stiffness (Fig. 5, *A* and *B*) started increasing at ~60 s after the exchange of solutions. The brown areas of Fig. 5, *A* and *B* show that the stiffness increase was first within the frequency range of 5–15 Hz and then extended to the range of 5–20 Hz as time after cell activation increased. Similarly, the phase angle (Fig. 5, *C* and *D*) started increasing after the solution exchange, but the major increase began at ~60 s and the increase in phase angle also expanded from the range of 5–15 Hz to the range of 5–24 Hz (*white areas* of Fig. 5, *C* and *D*). Both stiffness and phase angle of muscle cells reached a steady state at ~100 s after activation, or 40 s after stiffness and phase angle began to increase. The large stiffness and phase angle increases are consistent with the increase in the number of

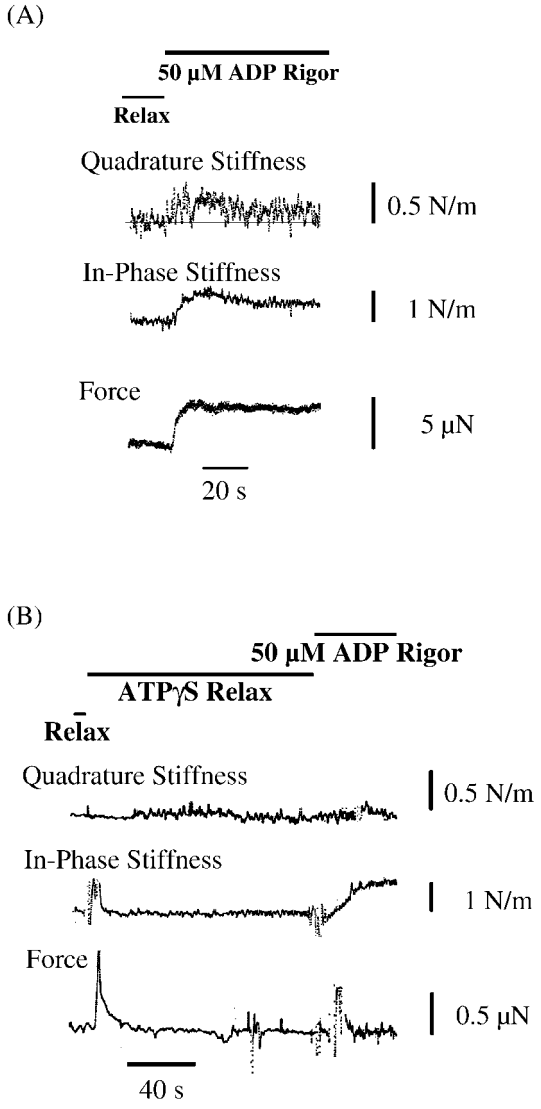

FIGURE 4 (*A*) The changes of the quadrature stiffness, in-phase stiffness, and force of a muscle cell when the bathing solution was changed from relaxing solution to 50 μM ADP rigor solution. (*B*) The changes of the quadrature stiffness, in-phase stiffness, and force of a muscle cell when the bathing solution was first changed from relaxing solution to ATPγS relaxing solution, and then 50 μM ADP rigor solution.

attached cycling cross-bridges, and the extension of the frequency response to higher frequencies indicates an increase in cross-bridge cycling rate. To increase the temporal resolution for the continuous traces of stiffness and phase angle (Fig. 5), frequency responses were not averaged over five measurements, but rather smoothed by the 10-point binomial method. Stiffness data below 5 Hz had high noise levels, and thus data of muscle stiffness at frequencies lower than 5 Hz were not displayed. The negative phase angles around 5 Hz (*green spots* in Fig. 5 *C*) are much smaller than those in Figs. 3 and 6. This is due to the difference in the methods of signal processing (see Methods). During the smoothing process of these spectrums, the large and sharp negative phase angle was averaged with adjacent points.

Force maintenance was reached at 100 s of activation, or 40 s after stiffness and phase angle began to increase. During force maintenance (Fig. 6), the mean (*solid line,* $n = 9$) of the normalized stiffness increased with frequency to a level of $\sim$0.7 at 5 Hz, then remained relatively constant until 14 Hz, after which it began to decrease and became lower than the passive stiffness at $\sim$18 Hz. The mean (*solid line,* $n = 4$) of the phase angles decreased with frequency to $-150°$ at 5 Hz, then rapidly increased to 180° at 8 Hz, followed by a slow decrease until a sudden 100° drop at 22 Hz, and finally a slow decrease. The frequency responses of muscle stiffness were consistent among muscle cells, as indicated by the small standard deviation. The profile of the mean phase spectrum suggests that there are at least three exponential processes (indicated by 1, 2, and 3 in Fig. 6) in the cross-bridge cycle that contribute to this spectrum, and the second process is an energy-generating process (Kawai and Brandt, 1980). For each cell, stiffness and phase spectrums were referenced to those in the passive state and the stiffness was normalized to the peak stiffness between frequencies 10 and 20 Hz. The frequency responses recorded at 5, 10, 15, and 20 min after the initial continuous recording were similar to that recorded at 100 s after activation (Fig. 5).

DISCUSSION

In the present study we have demonstrated that the frequency response of muscle stiffness obtained during the increasing-frequency sinusoidal sequence is a promising method for studying the molecular mechanism of smooth muscle contraction. The sequences provide good temporal and frequency resolution, and their bandwidth and spectrum can be easily manipulated. The noise level on force trace and frequency response during the length perturbation was much lower than during the pseudo-random white noise length perturbation. Although the data in lower and higher frequencies are less accurate due to the environmental noise and instrumentation setup, the frequency responses of muscle stiffness are consistent among muscle cells. We have detected attached cross-bridges in the relaxed state and continuously monitored the frequency response of muscle stiffness in the active state with a 3-s temporal resolution.

Relaxed state

Smooth muscle cells could contain viscous elements that are broken and/or rearranged during the length changes we employed to produce the passive state. However, the prominent negative phase angles in the relaxed state (Fig. 3 *B*) suggests the existence of an energy-generating process. We can think of no other process in muscle that generates energy other than a population of attached cross-bridges. Although no stiffness increase over the passive state was observed, the existence of attached cross-bridges is also consistent with our results using low ADP rigor solution

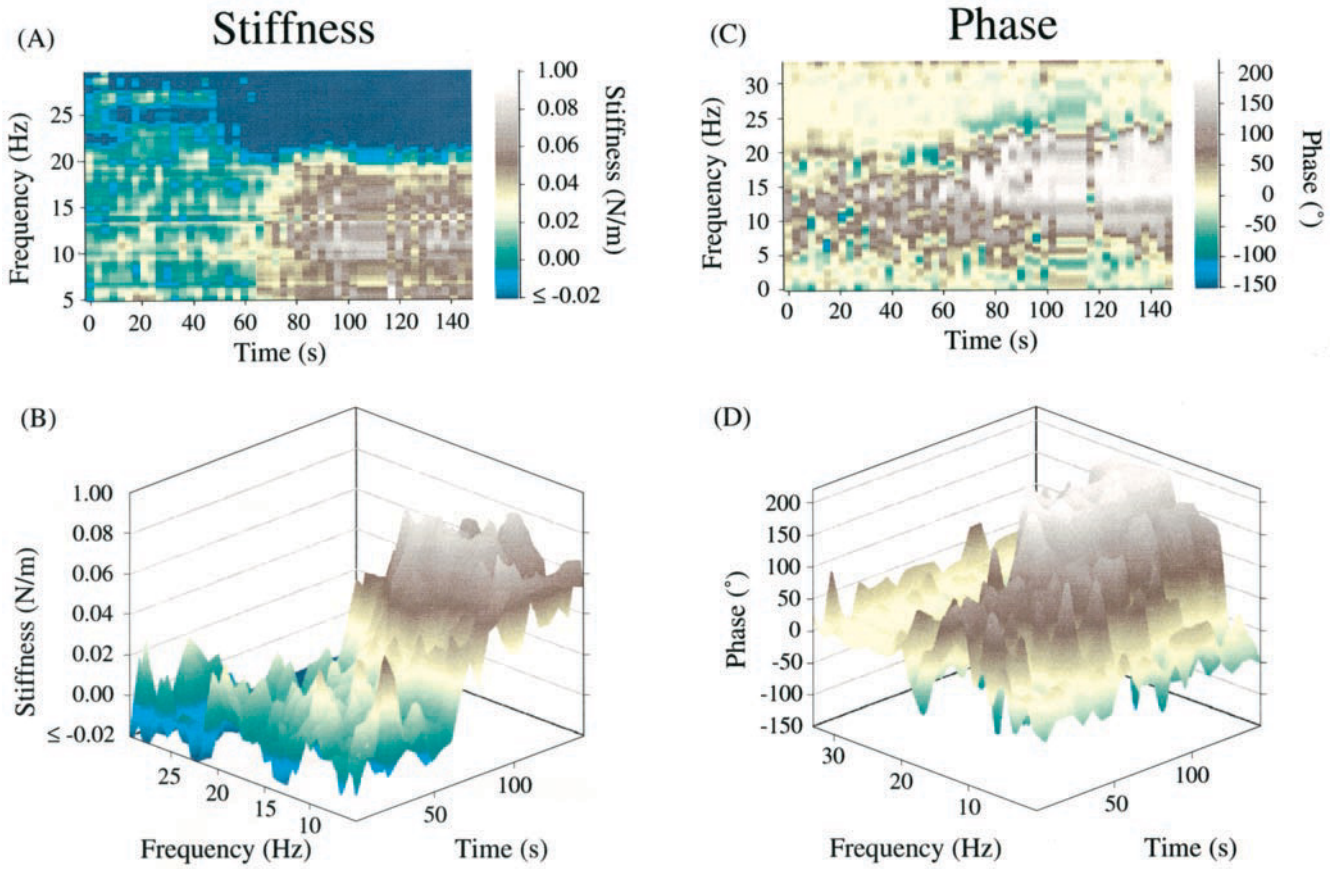

FIGURE 5 The time course of frequency response from the beginning of exchanging relaxing solution with activating solution. (*A*) and (*B*) are stiffness spectrums and (*C*) and (*D*) are phase spectrums. (*A*) and (*C*) are the top-view images of (*B*) and (*D*), respectively. The stiffness and phase angle were smoothed by a 10-point binomial method and referenced to those of the passive state. The amplitude scales of the stiffness and phase spectrums are shown with the Terrain color table as indicated by the vertical color legends in (*A*) and (*C*). The stiffness range shown is from −0.02 to 1 N/m; stiffness lower than −0.02 N/m is indicated by deep blue.

(Fig. 4). We would suggest that a population of attached AM and AMADP cross-bridges may exist in relaxed cells. Force would develop in ADP rigor solution as the ADP is converted to ATP (by intracellular creatine kinase and/or myokinase). The resulting low [ATP] would cause AM cross-bridge detachment. Coincident with the detachment of AM cross-bridges, AMADP cross-bridges would undergo a force producing isomerization, and increase both force and quadrature stiffness. AMADP cross-bridges could also promote the cooperative reattachment of dephosphorylated cross-bridges (Somlyo et al., 1988) resulting in an increase in in-phase stiffness. As intracellular phosphate stores are depleted, ATP would be depleted, and the cell would enter a high force rigor state (high in-phase stiffness, low quadrature stiffness). This hypothesis is supported by the observation that quadrature stiffness returns to baseline level after force develops (Fig. 4 *A*).

As another test for the existence of a population of attached cross-bridges in relaxed smooth muscle, ATPγS was used to eliminate attached cross-bridges. When cells were transferred from ATPγS relaxing solution to low ADP rigor solution (Fig. 4 *B*), in-phase stiffness increased, which is consistent with the formation of rigor (AM) cross-bridges. However, increases in force and quadrature stiffness were not observed. All of these results suggest that a population of attached AMADP cross-bridges are present in relaxed smooth muscle, and the force increase observed in low ADP rigor solution is due to these attached cross-bridges.

Jiang and Morgan (1987, 1989) found that phorbol ester stimulation can induce smooth muscle contraction without a change in the resting level of intracellular $[Ca^{2+}]$. Since no statistically significant change in intracellular $[Ca^{2+}]$ was detected during the contraction, a change in the resting level of MLC phosphorylation should not occur. Without an increase in MLC phosphorylation, no new cross-bridges should be formed. The phorbol ester induced contraction may rely on a population of AMADP cross-bridges present in relaxed smooth muscle. One can see from comparing the phase spectrums of the relaxed (Fig. 3 *B*) and active states (Fig. 6), the second process (marked with "2" in both Figs. 3 *B* and 6), which generates energy in the relaxed state, also exists in the active state. Thus, contractions that occur

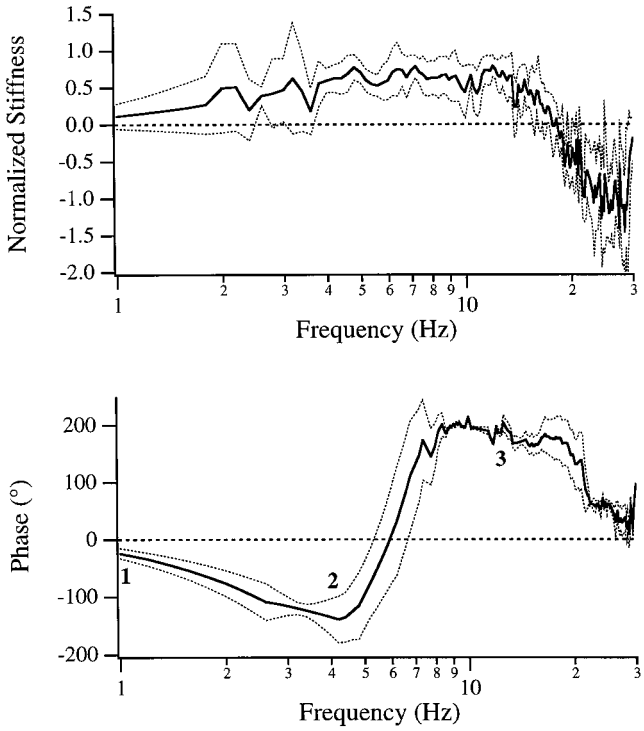

FIGURE 6 The mean (*solid line*) and standard deviation (*dotted lines*) of the frequency response during force maintenance (100 s after activation). The stiffness and phase spectrums were averaged over nine and four cells, respectively. The frequency response of each muscle cell was processed as described in Fig. 3.

without a change in the baseline level of $[Ca^{2+}]$ or MLC phosphorylation may depend on the presence of these attached cross-bridges, which could produce force in a cooperative manner (Somlyo et al., 1988). In addition, these cross-bridges may contribute to the molecular mechanism of force maintenance during stimulation of intact preparations after the MLC phosphorylation peaks.

Active state

As the muscle cell contracted, the stiffness and phase angle of cross-bridge cycling steadily increased. These increases extended to higher frequencies and then stabilized 100 s after activation, or 40 s after stiffness and phase angle began to increase (Fig. 5). The extension of the frequency response to higher frequencies suggests that certain processes within the cross-bridge cycling were getting faster as contraction progressed, but then remained stable during force maintenance. This is in contrast to observations based on V_{max} (Dillon and Murphy, 1982; Moreland et al., 1987), where cross-bridge cycling became slower during force maintenance. V_{max} is determined by using either the slack test (Edman, 1979) or by extrapolation from the force versus velocity relationship (Dillon and Murphy, 1982). For the slack test, V_{max} shows how fast the muscle length changes after a sudden and large shortening step. For isotonic quick releases, muscle length is rapidly decreased to a length that drops the force to a new level, and the resulting changes in muscle length that are required to maintain the set force are used to compute the velocity. Clamping the force to a new, lower level requires a rapid shortening of the muscle; the lower the load, the larger the length step. Both techniques for determining V_{max} include a sudden decrease in muscle length that will lead to a redistribution of cross-bridge states, and to a change in the distribution of cross-bridges in the ATPase cycle. The time course of the resulting muscle length change represents the sum of all these changes rather than a direct representation of the cross-bridge cycling rate. The length perturbation sequence we used in the present study of single cells has much smaller amplitude (~0.6–0.8% of a cell length) and thus the disturbance to the system is small. Compared to the measurement of V_{max}, data from the continuously monitored frequency response of the muscle stiffness reveal a more complete description of the rate changes within the cross-bridge cycle during muscle contraction.

In the present study, single skinned smooth muscle cells were activated with Ca^{2+}. This closely mimics the Ca^{2+} transient observed with <90 mM KCl depolarization (Bradley and Morgan, 1987), and our results provide a clear picture of the cross-bridge cycling rate during force maintenance for these contractions. We may not have observed slowing of cross-bridge cycling rate in our experiments for several reasons. Since MLC phosphorylation remains constant for Ca^{2+}-activated skinned muscle (Zhang and Moreland, 1994), slowing of cross-bridge cycling rate during force maintenance may not occur. However, Moreland et al. (1987) demonstrated during contractions stimulated with 40 mM KCl depolarization that even though MLC phosphorylation remained constant during the contraction, V_{max} sharply increased and then decreased to a lower steady level (~75% of the peak V_{max}) during force maintenance. In our studies of single cells, if the decrease in the cross-bridge cycling rate is similar to that reported by Moreland et al. (1987), we should have detected a shift in the spectrums of stiffness and phase to lower frequencies during force maintenance (Fig. 5). There are ripples in the time course of frequency response plots (Fig. 5) and thus small changes in the frequency response would be difficult to detect.

During force maintenance, the general profiles of frequency response (Fig. 6) are similar to those from myocardium (Kawai et al., 1993) and skeletal muscle fibers (Kawai and Brandt, 1980; Wang and Kawai, 1996), but the profiles shifted to lower frequencies since smooth muscle contraction is slower than that of skeletal muscle or myocardium. The frequency response of single smooth muscle cells in the present study reveals that there are at least three exponential processes of the cross-bridge cycle contributing to force maintenance instead of two processes, as suggested by others (Hai and Murphy, 1988; Vyas et al., 1994). The third process was recruited after the muscle cell was activated.

The amplitude of the phase spectrum is about three times larger than those reported by Kawai's group. Besides being a different muscle type, the larger amplitude of phase spec-

trum may be due to the size or composition of tissue. In our laboratory, the activation of portal vein strips produces a phase angle of ~8° (unpublished observation). Since strips of tissue contain connective tissues and cells, the phase angle of each cell may be reduced.

The negative stiffness at higher frequencies (Fig. 6) indicates that the active stiffness is lower than the passive stiffness. This is not due to the change in the kinetics of cross-bridge cycling since all attached cross-bridges should have positive stiffness, and there were no attached cross-bridges in the passive state. When the stiffness of the active state (Fig. 6) falls below zero at frequencies higher than 18 Hz, the total stiffness is not negative, but rather falls below that of the passive state at these frequencies. This could be the result of the vibration of the capillary tube decreasing as the stiffness of the cell increases, which leads to a fall in the apparent cell stiffness.

Further studies

Kawai and Brandt (1980) have identified three processes (or apparent rate constants) in skeletal muscle with the plots of stiffness versus frequency obtained from several fixed-frequency sine wave measurements. Changes in the relative population of cross-bridge states affect the shape of the frequency response. For example, by decreasing ATP or increasing Pi, the relative population of the AM or AMADP · Pi states is increased (Kawai et al., 1993), and the profile of frequency response has been demonstrated to have a slight leftward shift (to lower frequencies). In addition, the shape of frequency response is unique for skinned fibers in low ATP, high ADP, or high Pi.

In current studies we have observed the increase and extent of stiffness and phase angle as muscle-contracted, but we cannot identify the steps of the cross-bridge cycle that cause the change. To study the molecular mechanism of force maintenance in smooth muscle, it is necessary to deduce a model of cross-bridge cycling from the frequency responses of each attached cross-bridge step (e.g., AMADP, AMADP · Pi, and AM) and known kinetic constants of the elementary steps. With the developed model we can study smooth muscle contraction using two different approaches. First, the changes of elementary steps with muscle contraction can be investigated by tracking the time course of each elementary step in cross-bridge cycling from the beginning of muscle contraction. Second, the differences in cross-bridge cycling in response to different types of activation (i.e., agonist activation, KCl depolarization, and stimulation with phorbol esters) can be studied by comparing the time courses of attached cross-bridge states or the profiles of stiffness and phase during muscle contraction.

We thank Dr. Pepe Whittenbery for his support of the mechanical apparatus and electronics systems.

This work was supported by National Heart, Lung, and Blood Institute Grant HL44181 and National Institutes of Health Training Grant T32HL07653 (to G.S.).

REFERENCES

Bialojan, C., J. C. Reugg, and J. DiSalvo. 1987. A myosin phosphatase modulates contractility in skinned smooth muscle. *Pflügers Arch.* 410: 304–312.

Bradley, A. B., and K. G. Morgan. 1987. Alterations in cytoplasmic calcium sensitivity during porcine coronary artery contractions as detected by aequorin. *J. Physiol.* 385:437–448.

Brozovich, F. V., and M. Yamakawa. 1995. Thin filament regulation of force activation is not essential in single α-toxin permeabilized vascular smooth muscle. *Am. J. Physiol.* 268:C237–C242.

Butler, T. M., M. J. Siegman, and S. U. Mooers. 1986. Slowing of cross-bridge cycling in smooth muscle without evidence of an internal load. *Am. J. Physiol.* 251:C945–C950.

Dillon, P. F., M. O. Aksoy, S. P. Driska, and R. A. Murphy. 1981. Myosin phosphorylation and the cross bridge cycle in arterial smooth muscle. *Science*. 211:495–497.

Dillon, P. F., and R. A. Murphy. 1982. Tonic force maintenance with reduced shortening velocity in arterial smooth muscle. *Am. J. Physiol.* 242:C102–C108.

Edman, K. A. P. 1979. The velocity of unloaded shortening and its relation to sarcomere length and isometric force in vertebrate muscle fibers. *J. Physiol. (Lond.)* 291:143–159.

Goldman, Y. E., M. G. Hibberd, and D. R. Trentham. 1984a. Relaxation of rabbit psoas muscle fibers from rigor by photochemical generation of adenosine-5′-triphosphate. *J. Physiol.* 354:577–604.

Goldman, Y. E., M. G. Hibberd, and D. R. Trentham. 1984b. Initiation of active contraction by photogeneration of adenosine-5′-triphosphate in rabbit psoas muscle fibers. *J. Physiol.* 354:605–624.

Goody, R. S., and W. Hofmann. 1980. Stereochemical aspects of the interaction of myosin and actomyosin with nucleotides. *J. Muscle Res. Cell Motil.* 1:101–115.

Haeberle, J. R., D. R. Hathaway, and A. A. DePaoli-Roach. 1985. Dephosphorylation of myosin by the catalytic subunit of a type-2 phosphatase produces relaxation of chemically skinned uterine smooth muscle. *J. Biol. Chem.* 260:9965–9968.

Hai, C. M., and R. A. Murphy. 1988. Cross-bridge phosphorylation and regulation of latch state in smooth muscle. *Am. J. Physiol.* 254: C99–C106.

Hartshorne, D. J. 1987. Biochemistry of the contractile process in smooth muscle. *In* Physiology of the Gastrointestinal Tract, 2nd ed. L. R. Johnson, editor. Raven Press, New York. 423–482.

Jiang, M. J., and K. G. Morgan. 1987. Intracellular calcium levels in phorbol ester-induced contractions of vascular smooth muscle. *Am. J. Physiol.* 253:H1365–H1371.

Jiang, M. J., and K. G. Morgan. 1989. Agonist specific myosin phosphorylation and intracellular calcium during isometric contractions of vascular muscle. *Pflügers Arch.* 413:637–643.

Kamm, K. E., and J. T. Stull. 1985. The function of myosin and myosin light chain kinase phosphorylation in smooth muscle. *Annu. Rev. Pharmacol. Toxicol.* 25:593–620.

Kawai, M., and P. W. Brandt. 1980. Sinusoidal analysis: a high resolution method for correlating biochemical reactions with physiological processes in activated skeletal muscles of rabbit, frog and crayfish. *J. Muscle Res. Cell Motil.* 1:279–603.

Kawai, M., Y. Saeki, and Y. Zhao. 1993. Cross-bridge scheme and the kinetic constants of elementary steps deduced from chemically skinned papillary and trabecular muscles of the ferret. *Circ. Res.* 73:35–50.

Moreland, S., R. S. Moreland, and H. A. Singer. 1987. Apparent dissociation between myosin light chain phosphorylation and maximal velocity of shortening in KCl depolarized swine carotid artery: effect of temperature and KCl concentration. *Pflügers Arch.* 408:139–145.

Somlyo, A. V., Y. E. Goldman, T. Fujimori, M. Bond, D. R. Trentham, and

A. P. Somlyo. 1988. Crossbridge kinetics, cooperativity and negatively strained cross bridges in vertebrate smooth muscle: a laser flash photolysis study. *J. Gen. Physiol.* 91:165–192.

Vyas T. B., S. U. Mooers, S. R. Narayan, M. J. Siegman, and R. M. Butler. 1994. Cross-bridge cycling at rest and during activation. *J. Biol. Chem.* 269:7316–7322.

Wang, G., and M. Kawai. 1996. Effects of MgATP and MgADP on the cross-bridge kinetics of rabbit soleus slow-twitch muscle fibers. *Biophys. J.* 71:1450–1461.

Zhang, Y., and R. S. Moreland. 1994. Regulation of Ca^{2+}-dependent ATPase activity in detergent-skinned vascular smooth muscle. *Am. J. Physiol.* 267:H1032–H1039.